

University of Nebraska - Lincoln

DigitalCommons@University of Nebraska - Lincoln

Kenneth Bloom Publications

Research Papers in Physics and Astronomy

5-16-1998

Search for Inclusive $b \rightarrow s l^+ l^-$

S. Glenn

University of Rochester, Rochester, New York

Kenneth A. Bloom

University of Nebraska-Lincoln, kenbloom@unl.edu

CLEO Collaboration

Follow this and additional works at: <https://digitalcommons.unl.edu/physicsbloom>



Part of the [Physics Commons](#)

Glenn, S.; Bloom, Kenneth A.; and Collaboration, CLEO, "Search for Inclusive $b \rightarrow s l^+ l^-$ " (1998). *Kenneth Bloom Publications*. 152.

<https://digitalcommons.unl.edu/physicsbloom/152>

This Article is brought to you for free and open access by the Research Papers in Physics and Astronomy at DigitalCommons@University of Nebraska - Lincoln. It has been accepted for inclusion in Kenneth Bloom Publications by an authorized administrator of DigitalCommons@University of Nebraska - Lincoln.

Search for Inclusive $b \rightarrow sl^+l^-$

S. Glenn,¹ S.D. Johnson,¹ Y. Kwon,^{1,*} S. Roberts,¹ E.H. Thorndike,¹ C.P. Jessop,² K. Lingel,² H. Marsiske,² M.L. Perl,² V. Savinov,² D. Ugolini,² R. Wang,² X. Zhou,² T.E. Coan,³ V. Fadeyev,³ I. Korolkov,³ Y. Maravin,³ I. Narsky,³ V. Shelkov,³ J. Staeck,³ R. Stroynowski,³ I. Volobouev,³ J. Ye,³ M. Artuso,⁴ A. Efimov,⁴ M. Goldberg,⁴ D. He,⁴ S. Kopp,⁴ G.C. Moneti,⁴ R. Mountain,⁴ S. Schuh,⁴ T. Skwarnicki,⁴ S. Stone,⁴ G. Viehhauser,⁴ X. Xing,⁴ J. Bartelt,⁵ S.E. Csorna,⁵ V. Jain,^{5,†} K.W. McLean,⁵ S. Marka,⁵ R. Godang,⁶ K. Kinoshita,⁶ I.C. Lai,⁶ P. Pomianowski,⁶ S. Schrenk,⁶ G. Bonvicini,⁷ D. Cinabro,⁷ R. Greene,⁷ L.P. Perera,⁷ G.J. Zhou,⁷ B. Barish,⁸ M. Chadha,⁸ S. Chan,⁸ G. Eigen,⁸ J.S. Miller,⁸ C. O'Grady,⁸ M. Schmidtler,⁸ J. Urheim,⁸ A.J. Weinstein,⁸ F. Würthwein,⁸ D.W. Blis,⁹ G. Masek,⁹ H.P. Paar,⁹ S. Prell,⁹ V. Sharma,⁹ D.M. Asner,¹⁰ J. Gronberg,¹⁰ T.S. Hill,¹⁰ D.J. Lange,¹⁰ S. Menary,¹⁰ R.J. Morrison,¹⁰ H.N. Nelson,¹⁰ T.K. Nelson,¹⁰ C. Qiao,¹⁰ J.D. Richman,¹⁰ D. Roberts,¹⁰ A. Ryd,¹⁰ M.S. Witherell,¹⁰ R. Balest,¹¹ B.H. Behrens,¹¹ W.T. Ford,¹¹ H. Park,¹¹ J. Roy,¹¹ J.G. Smith,¹¹ J.P. Alexander,¹² C. Bebek,¹² B.E. Berger,¹² K. Berkelman,¹² K. Bloom,¹² D.G. Cassel,¹² H.A. Cho,¹² D.S. Crowcroft,¹² M. Dickson,¹² P.S. Drell,¹² K.M. Ecklund,¹² R. Ehrlich,¹² A.D. Foland,¹² P. Gaidarev,¹² L. Gibbons,¹² B. Gittelman,¹² S.W. Gray,¹² D.L. Hartill,¹² B.K. Heltsley,¹² P.I. Hopman,¹² J. Kandaswamy,¹² P.C. Kim,¹² D.L. Kreinick,¹² T. Lee,¹² Y. Liu,¹² N.B. Mistry,¹² C.R. Ng,¹² E. Nordberg,¹² M. Ogg,^{12,‡} J.R. Patterson,¹² D. Peterson,¹² D. Riley,¹² A. Soffer,¹² B. Valant-Spaight,¹² C. Ward,¹² M. Athanas,¹³ P. Avery,¹³ C.D. Jones,¹³ M. Lohner,¹³ C. Prescott,¹³ J. Yelton,¹³ J. Zheng,¹³ G. Brandenburg,¹⁴ R.A. Briere,¹⁴ A. Ershov,¹⁴ Y.S. Gao,¹⁴ D.Y.-J. Kim,¹⁴ R. Wilson,¹⁴ H. Yamamoto,¹⁴ T.E. Browder,¹⁵ Y. Li,¹⁵ J.L. Rodriguez,¹⁵ T. Bergfeld,¹⁶ B.I. Eisenstein,¹⁶ J. Ernst,¹⁶ G.E. Gladding,¹⁶ G.D. Gollin,¹⁶ R.M. Hans,¹⁶ E. Johnson,¹⁶ I. Karliner,¹⁶ M.A. Marsh,¹⁶ M. Palmer,¹⁶ M. Selen,¹⁶ J.J. Thaler,¹⁶ K.W. Edwards,¹⁷ A. Bellerive,¹⁸ R. Janicek,¹⁸ D.B. MacFarlane,¹⁸ P.M. Patel,¹⁸ A.J. Sadoff,¹⁹ R. Ammar,²⁰ P. Baringer,²⁰ A. Bean,²⁰ D. Besson,²⁰ D. Coppage,²⁰ C. Darling,²⁰ R. Davis,²⁰ N. Hancock,²⁰ S. Kotov,²⁰ I. Kravchenko,²⁰ N. Kwak,²⁰ S. Anderson,²¹ Y. Kubota,²¹ S.J. Lee,²¹ J.J. O'Neill,²¹ S. Patton,²¹ R. Poling,²¹ T. Riehle,²¹ A. Smith,²¹ M.S. Alam,²² S.B. Athar,²² Z. Ling,²² A.H. Mahmood,²² H. Severini,²² S. Timm,²² F. Wappler,²² A. Anastassov,²³ J.E. Duboscq,²³ D. Fujino,^{23,§} K.K. Gan,²³ T. Hart,²³ K. Honscheid,²³ H. Kagan,²³ R. Kass,²³ J. Lee,²³ M.B. Spencer,²³ M. Sung,²³ A. Undrus,^{23,||} R. Wanke,²³ A. Wolf,²³ M.M. Zoeller,²³ B. Nemati,²⁴ S.J. Richichi,²⁴ W.R. Ross,²⁴ P. Skubic,²⁴ M. Bishai,²⁵ J. Fast,²⁵ J.W. Hinson,²⁵ N. Menon,²⁵ D.H. Miller,²⁵ E.I. Shibata,²⁵ I.P.J. Shipsey,²⁵ and M. Yurko²⁵

(CLEO Collaboration)

¹University of Rochester, Rochester, New York 14627²Stanford Linear Accelerator Center, Stanford University, Stanford, California 94309³Southern Methodist University, Dallas, Texas 75275⁴Syracuse University, Syracuse, New York 13244⁵Vanderbilt University, Nashville, Tennessee 37235⁶Virginia Polytechnic Institute and State University, Blacksburg, Virginia 24061⁷Wayne State University, Detroit, Michigan 48202⁸California Institute of Technology, Pasadena, California 91125⁹University of California, San Diego, La Jolla, California 92093¹⁰University of California, Santa Barbara, California 93106¹¹University of Colorado, Boulder, Colorado 80309-0390¹²Cornell University, Ithaca, New York 14853¹³University of Florida, Gainesville, Florida 32611¹⁴Harvard University, Cambridge, Massachusetts 02138¹⁵University of Hawaii at Manoa, Honolulu, Hawaii 96822¹⁶University of Illinois, Champaign-Urbana, Illinois 61801¹⁷Carleton University, Ottawa, Ontario, Canada K1S 5B6 and the Institute of Particle Physics, Canada¹⁸McGill University, Montréal, Québec, Canada H3A 2T8 and the Institute of Particle Physics, Canada¹⁹Ithaca College, Ithaca, New York 14850²⁰University of Kansas, Lawrence, Kansas 66045²¹University of Minnesota, Minneapolis, Minnesota 55455²²State University of New York at Albany, Albany, New York 12222²³Ohio State University, Columbus, Ohio 43210²⁴University of Oklahoma, Norman, Oklahoma 73019

²⁵Purdue University, West Lafayette, Indiana 47907
(Received 1 October 1997)

We have searched for the effective flavor changing neutral-current decays $b \rightarrow sl^+l^-$ using an inclusive method. We set upper limits on the branching ratios $\mathcal{B}(b \rightarrow se^+e^-) < 5.7 \times 10^{-5}$, $\mathcal{B}(b \rightarrow s\mu^+\mu^-) < 5.8 \times 10^{-5}$, and $\mathcal{B}(b \rightarrow se^\pm\mu^\mp) < 2.2 \times 10^{-5}$ [at 90% confidence level (C.L.)]. Combining the dielectron and dimuon decay modes we find $\mathcal{B}(b \rightarrow sl^+l^-) < 4.2 \times 10^{-5}$ (at 90% C.L.). [S0031-9007(98)05533-1]

PACS numbers: 13.20.He, 11.30.Hv

Flavor changing neutral currents (FCNC) are forbidden to first order in the standard model. Second order loop diagrams, known as penguin and box diagrams, can generate effective FCNC which lead to $b \rightarrow s$ transitions. These processes are of considerable interest because they are sensitive to V_{ts} , the Cabibbo-Kobayashi-Maskawa matrix element which will be very difficult to measure in direct decays of the top quark. These processes are also sensitive to non-standard-model physics [1], since charged Higgs bosons, new gauge bosons, or supersymmetric particles can contribute via additional loop diagrams.

The electromagnetic penguin decay $b \rightarrow s\gamma$ was first observed by CLEO in the exclusive mode $B \rightarrow K^*\gamma$ with $\mathcal{B}(B \rightarrow K^*\gamma) = (4.2 \pm 0.8 \pm 0.6) \times 10^{-5}$ [2]. The inclusive rate for the decay $B \rightarrow X_s\gamma$ was measured to be $\mathcal{B}(b \rightarrow s\gamma) = (2.32 \pm 0.57 \pm 0.35) \times 10^{-4}$ [3]. The measured inclusive $b \rightarrow s\gamma$ rate is consistent with standard model calculations.

The $b \rightarrow sl^+l^-$ decay rate is expected in the standard model to be nearly 2 orders of magnitude lower than the rate for $b \rightarrow s\gamma$ decays. Nevertheless, the $b \rightarrow sl^+l^-$ process has received considerable attention since it offers a deeper insight into the effective Hamiltonian describing FCNC processes in B decays [4]. While $b \rightarrow s\gamma$ is only sensitive to the absolute value of the C_7 Wilson coefficient in the effective Hamiltonian, $b \rightarrow sl^+l^-$ is also sensitive to the sign of C_7 and to the C_9 and C_{10} coefficients, where the relative contributions vary with l^+l^- mass. These three coefficients are related to three different processes contributing to $b \rightarrow sl^+l^-$: electromagnetic and electroweak penguins, and a box diagram. Processes beyond the standard model can alter both the magnitude and the sign of the Wilson coefficients. The higher-order QCD corrections for $b \rightarrow sl^+l^-$ are smaller than for the electromagnetic penguin and have been calculated in next-to-leading order [5,6].

Several experiments (UA1 [7], CLEO [8], and CDF [9]) have searched for the exclusive decays $B \rightarrow Kl^+l^-$ and $B \rightarrow K^*l^+l^-$ and set upper limits at the level of $(1 - 2) \times 10^{-5}$ at 90% confidence level (C.L.). These exclusive final states are expected to constitute about 6% and 15% of the inclusive $X_sl^+l^-$ rate, respectively [10]. Inclusively measured rates are more interesting because they can be directly related to underlying quark transitions without large theoretical uncertainties in formation probabilities for specific hadronic final states. Combining electron and muon modes, the previous generation of the CLEO experiment set an inclusive limit: $\mathcal{B}(b \rightarrow$

$sl^+l^-) < 1.2 \times 10^{-3}$ (90% C.L.) [11]. The UA1 experiment [7] searched for inclusive $b \rightarrow s\mu^+\mu^-$ at the end point of the dilepton mass distribution [$M(\mu^+\mu^-) > 3.9$ GeV] which comprises about a tenth of the total rate. Extrapolating to the full phase space, UA1 claims a limit of $< 5 \times 10^{-5}$ (90% C.L.). However, a simulation of the UA1 acceptance shows that UA1 overestimated their efficiency by at least a factor of 3 [12].

In this Letter, we present results of the search for inclusive $b \rightarrow s\mu^+\mu^-$, $b \rightarrow se^+e^-$, and $b \rightarrow se^\pm\mu^\mp$. The latter decay violates conservation of electron and muon lepton numbers and thus can originate only from processes beyond the standard model. The data were obtained with the CLEO II detector at the Cornell Electron Storage Ring. A sample with an integrated luminosity of 3.1 fb^{-1} was collected on the $\Upsilon(4S)$ resonance. This sample contains $(3.30 \pm 0.06) \times 10^6$ produced $B\bar{B}$ pairs. For background subtraction we also use 1.6 fb^{-1} of data collected just below the $\Upsilon(4S)$. CLEO II is a general purpose solenoidal spectrometer described in detail in Ref. [13].

The data selection method is very similar to the reconstruction method presented in our previous measurement of the $b \rightarrow s\gamma$ rate [3], with the γ candidate replaced by a lepton pair. We select events that pass general hadronic event criteria based on charged track multiplicity, visible energy, and location of the event vertex. The highest energy pair of oppositely charged leptons is then selected. Electron candidates are required to have an energy deposition in the calorimeter nearly equal to the measured momentum, and to have a specific ionization (dE/dx) in the drift chamber consistent with that expected for an electron. Muon candidates are identified as charged tracks with matching muon-detector hits at absorber depths of at least three nuclear interaction lengths. In the $\mu^+\mu^-$ channel, one muon is required to penetrate at least five interaction lengths. We then look for a combination of hadronic particles, denoted X_s , with a kaon candidate and 0–4 pions, which together with the selected lepton pair satisfy energy-momentum constraints for the B decay hypothesis $B \rightarrow X_sl^+l^-$. To quantify consistency with this hypothesis, we use

$$\chi_B^2 = \left(\frac{M_B - 5.279}{\sigma_M} \right)^2 + \left(\frac{E_B - E_{\text{beam}}}{\sigma_E} \right)^2,$$

where $M_B = \sqrt{E_{\text{beam}}^2 - P_B^2}$, E_B , P_B are the measured energy and momentum of the B candidate, and σ_M , σ_E are experimental errors on M_B and E_B estimated from the

detector resolution and beam energy spread. The kaon candidate is a charged track with dE/dx and time of flight (TOF) consistent with the kaon hypothesis, or a $K_S^0 \rightarrow \pi^+ \pi^-$ candidate identified by a displaced vertex and invariant mass cut. A pion candidate is a charged track with dE/dx and TOF consistent with the pion hypothesis, or a $\pi^0 \rightarrow \gamma\gamma$ candidate. At most one π^0 is allowed in the X_s combination. In each event, we pick the combination that minimizes overall χ^2 , which includes χ_B^2 together with contributions from dE/dx , TOF, and K_S^0 and π^0 mass deviations, where relevant.

To suppress continuum background we require the event to have $H_2/H_0 < 0.45$, where H_i are Fox-Wolfram moments [14]. We also require $|\cos \theta_H| < 0.8$, where θ_H is the angle between the thrust axis of the candidate B and the thrust axis of the rest of the event. To suppress $B\bar{B}$ background we require the mass of the X_s system to be less than 1.8 GeV. The dominant $B\bar{B}$ background comes from two semileptonic decays of B or D mesons, which produce the lepton pair with two undetected neutrinos. Since most signal events are expected to have zero or one neutrino, we also require the mass of the undetected system in the event to be less than 1.5 GeV. By excluding the mode with $X_s = K\pi^+\pi^-\pi^0$, we reduce the expected $B\bar{B}$ background by an additional 21% while reducing the signal efficiency by only 6%.

Figure 1 shows the dilepton mass $M(l^+l^-)$ for the events which pass the cuts previously described and the B consistency requirement $\chi_B^2 < 6$, in the on- and off-resonance data samples. Unlike the $b \rightarrow s\gamma$ analysis, the continuum background is small. The peaks at the ψ and ψ' masses that are observed in the on-resonance data are due to well known decays $B \rightarrow X_s \psi^{(\prime)}$, $\psi^{(\prime)} \rightarrow l^+l^-$ involving long distance interactions in formation of the $\psi^{(\prime)}$ resonances. Using cuts on $M(X_s)$ to identify K and K^* , we measure the branching ratios for $B \rightarrow K^{(*)}\psi^{(\prime)}$ and obtain results consistent with a recent CLEO publication [15]. For further analysis, we exclude events with $M(l^+l^-)$ near the ψ and ψ' masses (± 0.1 GeV for $\mu^+\mu^-$, $-0.3, +0.1$ GeV for e^+e^- , no cut for $e^\pm\mu^\pm$), since we want to probe short distance contributions to the production of $X_s l^+l^-$ states. The exclusion region is wider in the e^+e^- channel because of the radiative tail. After these cuts and continuum subtraction, we observe 10 ± 5 $X_s e^+e^-$, 12 ± 6 $X_s \mu^+\mu^-$, and 18 ± 8 $X_s e^\pm\mu^\pm$ events in the data, whereas from the Monte Carlo simulation of generic $B\bar{B}$ events we expect 9 ± 1 , 16 ± 2 , and 39 ± 3 (statistical errors only) background events, respectively. The generic $B\bar{B}$ Monte Carlo reproduces also the number of events in the tail of the χ_B^2 distribution ($6 < \chi_B^2 < 30$) where the signal contribution is expected to be 2.3 times smaller. Continuum-subtracted data yield 14 ± 6 , 26 ± 7 , and 66 ± 11 events, whereas the Monte Carlo expectations are 24 ± 2 , 29 ± 2 , and 71 ± 4 events, respectively. Therefore, no evidence for signal is found in the data and we proceed to set limits on these decay rates.

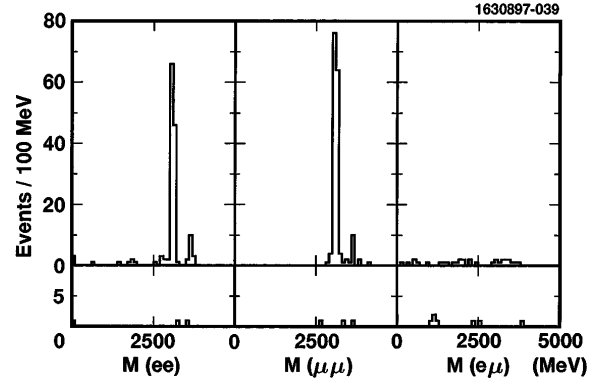


FIG. 1. $M(l^+l^-)$ distributions for the on- (upper) and off-resonance (lower) data with the $\chi_B^2 < 6$ cut. The scaling factor between the off- and on-resonance data is 1.9.

To avoid systematics related to absolute normalization of the $B\bar{B}$ Monte Carlo, instead of counting events after the $\chi_B^2 < 6$ cut, we loosen this cut to 30 and fit the observed χ_B^2 distributions in the on- and off-resonance data using a binned maximum likelihood method. We allow for signal contribution, as well as $B\bar{B}$ and continuum backgrounds. The relative normalization for continuum background between the on- and off-resonance data is fixed to the known ratio of integral luminosities and cross sections. The signal is expected to peak sharply at zero, whereas the backgrounds have flatter distributions [as an example, we show the expected signal and $B\bar{B}$ background shapes for the $X_s e^+e^-$ channel in Fig. 2(a)].

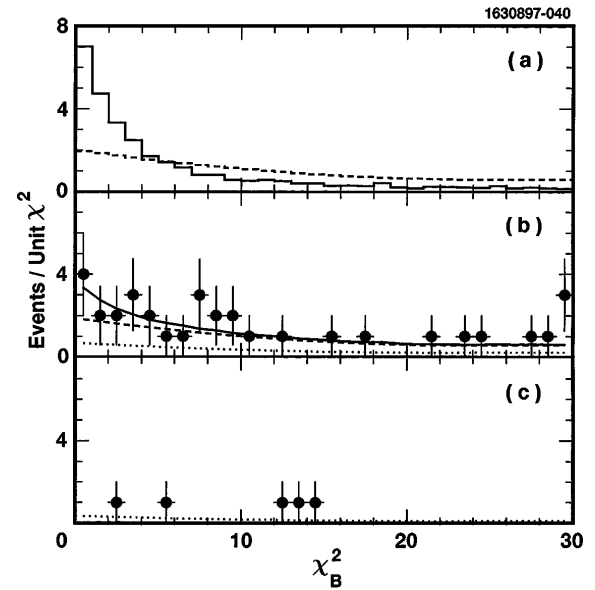


FIG. 2. χ_B^2 distributions for $X_s e^+e^-$ data. (a) The difference between the expected distribution for the signal (solid histogram) and $B\bar{B}$ background (dashed histogram). Both distributions are normalized to the same area. (b) The fit to the on-resonance data (points with error bars). The sum of all fitted contributions is indicated by a solid line. The fitted background contribution ($B\bar{B}$ plus continuum) is indicated by a dashed line. The estimated continuum background, indicated by a dotted line, is simultaneously constrained to the off-resonance data (c).

The shapes of all these contributions are fixed from the Monte Carlo simulation, while the normalizations are allowed to float. The Monte Carlo predictions for the signal shape distribution agree well with the distribution observed in the data for the $B \rightarrow \psi X_s$ signal. We assign a generous systematic error to the uncertainty in χ_B^2 signal and background shapes by varying X_s composition in the Monte Carlo as described below. The fitted number of $X_s e^+ e^-$, $X_s \mu^+ \mu^-$, and $X_s e^\pm \mu^\mp$ events is 7 ± 7 , 1 ± 7 , and -18 ± 10 , respectively. As an example, the fit to the $X_s e^+ e^-$ data is displayed in Fig. 2(b)–2(c).

To calculate the signal efficiency and to predict the χ_B^2 signal distribution we generated $b \rightarrow sl^+ l^-$ Monte Carlo events. The parton level distributions for $b \rightarrow se^+ e^-$ and $b \rightarrow s\mu^+ \mu^-$ are predicted from the effective Hamiltonian containing standard model contributions. The next-to-leading-order calculations were used [6]. At present, the effect of gluon bremsstrahlung on the outgoing s quark is only partially included in the theoretical calculations. After our ψ and ψ' veto cuts, the long distance interactions are expected to constructively interfere with the short distance contributions. Estimates of these interference effects are model dependent. The most recent calculation predicts modifications of the short distance rate by only about 2% [16] compared to 20% predicted by some earlier simplified models [17]. We neglect long distance interactions in our Monte Carlo. Since no theoretical calculations for the non-standard-model decay $b \rightarrow se^\pm \mu^\mp$ exist, we use a phase space model for these decays. To account for Fermi motion of the b quark inside the B meson we have used the spectator model by Ali *et al.* [18]. The particle content of the X_s system was modeled with the conventional method quark hadronization from JETSET [19]. For better accuracy of the simulations, when $M(X_s)$ is in the K or K^* mass region, the event is regenerated according to the theoretical predictions for the exclusive $B \rightarrow K^{(*)} l^+ l^-$ decays by Greub *et al.* [20]. The estimated efficiencies are 5.2%, 4.5%, and 7.3% for $e^+ e^-$, $\mu^+ \mu^-$, and $e^\pm \mu^\mp$ modes, respectively.

To estimate the systematic error due to the uncertainty in the χ_B^2 signal and background shapes, we divide the Monte Carlo sample into low and high multiplicity channels in the manner which produces the largest shape variation. This shape variation changes the upper limits by 9%, 19%, and 20% for the $e^+ e^-$, $\mu^+ \mu^-$, and $e^\pm \mu^\mp$ channels, respectively. Variations of the spectator model parameters [3] result in changes of the selection efficiency by $(12 \pm 4)\%$, $(30 \pm 4)\%$, and $(11 \pm 4)\%$, respectively. The larger uncertainty in the $\mu^+ \mu^-$ channel is the result of the lack of muon identification for $P_\mu < 1$ GeV/ c . Uncertainty in the modeling of the hadronization of the X_s system gives a contribution of 9%. Remaining systematic error in the simulation of detector response is dominated by charged tracking systematics and is estimated to be 14%. Adding all these sources of systematic errors in the quadrature, we estimate the total systematic errors to be 22%, 39%, and 28%, respectively.

Using a Gaussian likelihood integrated over positive signal values, we find upper limits using statistical errors only. We then loosen these limits by one unit of systematic uncertainty.

The final results are $\mathcal{B}(b \rightarrow se^+ e^-) < 5.7 \times 10^{-5}$, $\mathcal{B}(b \rightarrow s\mu^+ \mu^-) < 5.8 \times 10^{-5}$, and $\mathcal{B}(b \rightarrow se^\pm \mu^\mp) < 2.2 \times 10^{-5}$. The results are consistent with the standard model predictions [18], $(0.8 \pm 0.2) \times 10^{-5}$, $(0.6 \pm 0.1) \times 10^{-5}$, and 0, respectively. Combining the $e^+ e^-$ and $\mu^+ \mu^-$ results, we also set a limit on the rate averaged over lepton flavors, $\mathcal{B}(b \rightarrow sl^+ l^-) \equiv [\mathcal{B}(b \rightarrow se^+ e^-) + \mathcal{B}(b \rightarrow s\mu^+ \mu^-)]/2 < 4.2 \times 10^{-5}$ (90% C.L.).

The limit on $\mathcal{B}(b \rightarrow se^+ e^-)$ is more than an order of magnitude more restrictive than the previous limits. The limit on $\mathcal{B}(b \rightarrow s\mu^+ \mu^-)$ is also significantly tighter than the UA1 limit after correcting for the efficiency problem (see discussion above). Furthermore, in contrast with the UA1 measurement, the present analysis is sensitive to a much wider range of $M(l^+ l^-)$. Therefore, our extrapolation to the full phase space is more reliable, and we are sensitive to a broader range of processes beyond the standard model.

We gratefully acknowledge the effort of the CESR staff in providing us with excellent luminosity and running conditions. This work was supported by the National Science Foundation, the U.S. Department of Energy, the Heisenberg Foundation, the Alexander von Humboldt Stiftung, the Natural Sciences and Engineering Research Council of Canada, and the A. P. Sloan Foundation.

*Permanent address: Yonsei University, Seoul 120-749, Korea.

†Permanent address: Brookhaven National Laboratory, Upton, NY 11973.

‡Permanent address: University of Texas, Austin, TX 78712.

§Permanent address: Lawrence Livermore National Laboratory, Livermore, CA 94551.

||Permanent address: BINP, RU-630090 Novosibirsk, Russia.

- [1] See, for example, J. L. Hewett and J. D. Wells, Phys. Rev. D **55**, 5549 (1997); G. Burdman, Phys. Rev. D **52**, 6400 (1995); N. G. Deshpande, K. Panose, and J. Trampetić, Phys. Lett. B **308**, 322 (1993); W. S. Hou, R. S. Willey, and A. Soni, Phys. Rev. Lett. **58**, 1608 (1987).
- [2] CLEO Collaboration, R. Ammar *et al.*, Phys. Rev. Lett. **71**, 674 (1993); in *Proceedings of the 28th International Conference on High Energy Physics, Warsaw, Poland, 1996* (Report No. CLEO CONF 96-05).
- [3] CLEO Collaboration, M. S. Alam *et al.*, Phys. Rev. Lett. **74**, 2885 (1995).
- [4] A. Ali, T. Mannel, and T. Morozumi, Phys. Lett. B **273**, 505 (1991); A. Ali, G. F. Gudice, and T. Mannel, Z. Phys. C **67**, 417 (1995); J. L. Hewett, Phys. Rev. D **53**, 4964 (1996).
- [5] M. Misiak, Nucl. Phys. **B393**, 23 (1993); **439**, 461(E) (1995).

- [6] A. Buras and M. Münz, Phys. Rev. D **52**, 186 (1995).
- [7] UA1 Collaboration, C. Albajar *et al.*, Phys. Lett. B **262**, 163 (1991).
- [8] CLEO Collaboration, R. Balest *et al.*, in *Proceedings of the 27th International Conference on High Energy Physics, Glasgow, Scotland, 1994*, edited by P.J. Bussey and I.G. Knowles (IOP, London, 1995) (Report No. CLEO CONF 94-4).
- [9] CDF Collaboration, F. Abe *et al.*, Phys. Rev. Lett. **76**, 4675 (1996).
- [10] We have estimated a fraction of Kl^+l^- and $K^*l^+l^-$ final states among all $X_sl^+l^-$ decays by integrating the $1/\Gamma d\Gamma/dM(X_s)$ distribution predicted by the inclusive theoretical model described below in the appropriate $M(X_s)$ ranges.
- [11] CLEO Collaboration, A. Bean *et al.*, Phys. Rev. D **35**, 3533 (1987).
- [12] To simulate the UA1 acceptance, we use the PYTHIA program [19] to generate $p\bar{p} \rightarrow b\bar{b}X$ at 630 GeV in the center of mass energy. The simulation of $b \rightarrow s\mu^+\mu^-$ decays is described later in the text. For the kinematic cuts used by UA1 [$P_t(\mu) > 3$ GeV/c, $P_t(\mu^+\mu^-) > 7$ GeV/c, and $3.9 < M(\mu^+\mu^-) < 4.4$ GeV/ c^2], we obtain an efficiency of $(0.36 \pm 0.03)\%$ when normalized to b quark production with $P_t(b) > 6$ GeV/c and $|y(b)| < 1.5$. Further losses are expected due to inefficiencies in the trigger and reconstruction. The overall efficiency quoted in the UA1 publication [7] for these cuts and this normalization is three times larger: $(1.1 \pm 0.3)\%$. A large portion of this disagreement can be traced to the simulation of $M(\mu^+\mu^-)$ distribution in $B \rightarrow X_s\mu^+\mu^-$ decays. When applied to $B^0 \rightarrow \mu^+\mu^-$, our simulation of the UA1 kinematic cuts gives an acceptance consistent with the overall efficiency quoted by UA1. Furthermore, while our simulation of $B \rightarrow X_s\mu^+\mu^-$ decays predict that only $(6.7 \pm 0.6)\%$ of events passing the P_t cuts fall into the $3.9 < M(\mu^+\mu^-) < 4.4$ GeV/ c^2 interval, the number extracted from Table I in the UA1 paper is 2.3 times larger: $(15.0 \pm 0.3)\%$. The $M(\mu^+\mu^-)$ distribution generated by our Monte Carlo program is in good agreement with the distribution published by A. Ali *et al.* [18].
- [13] CLEO Collaboration, Y. Kubota *et al.*, Nucl. Instrum. Methods Phys. Res., Sect. A **320**, 66 (1992).
- [14] G. Fox and S. Wolfram, Phys. Rev. Lett. **41**, 1581 (1978).
- [15] CLEO Collaboration, C.S. Jessop *et al.*, Phys. Rev. Lett. **79**, 4533 (1997).
- [16] M.R. Ahmady, Phys. Rev. D **53**, 2843 (1996).
- [17] C.S. Lim, T. Morozumi, and A.I. Sanda, Phys. Lett. B **218**, 343 (1989); N.G. Deshpande, J. Trampetic, and K. Panose, Phys. Rev. D **39**, 1461 (1989); P.J. O'Donnell and H.K.K. Tung, Phys. Rev. D **43**, R2067 (1991); N. Paver and Riazuddin, Phys. Rev. D **45**, 978 (1992).
- [18] A. Ali, G. Hiller, L.T. Handoko, and T. Morozumi, Phys. Rev. D **55**, 4105 (1997).
- [19] T. Sjostrand, Comput. Phys. Commun. **82**, 74 (1994).
- [20] C. Greub, A. Ioannisian, and D. Wyler, Phys. Lett. B **346**, 149 (1995).